

Hydrodynamic equations and near critical large deviations of active lattice gases

Luke Neville

School of Mathematics, Fry Building, University of Bristol, BS8 1UG, United Kingdom

E-mail: luke.neville@bristol.ac.uk

Abstract. Using a path integral approach, we derive and study the hydrodynamic equations and large deviation functions for three active lattice gases. After a review of the path integral for master equations, we first look at a one dimensional model of motility induced phase separation (MIPS), re-deriving the large deviation function that was previously found through a mapping to the ABC model. After extracting the deterministic hydrodynamic equations from the large deviation function, we analyse them perturbatively near the MIPS critical point using a weakly non-linear analysis. Doing this we show that they reduce to equilibrium Model B very close to criticality, with non-equilibrium, or Active Model B+ terms emerging as we leave the critical region. The same type of weakly non-linear analysis is then applied to the full large deviation function, and we show that the near critical stationary probability distribution is given by the exponential of a ϕ^4 free energy, as expected in ordinary equilibrium phase separation. Similar calculations are then done for the two other lattice gases, one of flocking, and another MIPS model, and in both cases we find analogous results.

1. Introduction

Motile active matter consists of self-propelling particles that keep moving by constantly converting chemical energy into useful work [1–4]. This breaking of detailed balance means that they show behaviour that equilibrium thermodynamics would forbid, like phase separation in the presence of repulsive interactions [5–7], or the formation of flocks in two dimensions [8, 9]. Although originally discovered in agent based simulations [9], these effects are now best understood through the use of continuous hydrodynamic equations [2, 3, 10, 11]. Similar to equilibrium, this approach uses symmetry to pick out the hydrodynamic variables, before phenomenologically constructing dynamical equations governing their slow evolution in space and time [8, 12–14]. Because the resulting equations are ambivalent to microscopic detail, they can give great insight into universal properties like scaling exponents [15–17].

Despite this, it has always been desirable to connect these active hydrodynamic theories to microscopic models through coarse graining. The reason for this is two-fold. One, it helps to understand the range of validity of these equations, e.g. are

they accurate everywhere or perhaps only near critical points [12, 18]. And two, it gives information about the transport coefficients, telling us, say, whether they should be positive or negative. In the case of active, or motility induced phase separation (MIPS), this connection was achieved early on [10, 19]. The hydrodynamics matches the microscopic simulations quantitatively well, even being able to predict the binodals, or phase separated densities [20, 21]. Although discovered first, the situation is somewhat worse for flocking, where, although the hydrodynamic equations can be derived [17, 22–25], the predicted parameter values do not quantitatively match particle based simulations. The reason for this discrepancy comes from the number of uncontrolled approximations made in the derivation [21, 24]. For example, many of these derivations rely on a truncation of an infinite hierarchy of PDEs, an approximation that cannot be justified a priori [17].

Given these difficulties it seems necessary to find models that can be coarse grained in a mathematically controlled way, and a class that seems to fill this requirement is the diffusive lattice gas [26–28]. These stochastic models originated in the mathematical physics literature [29–32], and although often applied to boundary driven equilibrium systems [33], they have recently been applied to *internally* driven active matter [34–36]. Although perhaps more artificial than particle based simulations, they are valuable because they can be ‘exactly’ coarse grained into hydrodynamic equations. Of particular interest to us is the 2018 work by *Kourbane et al.* [37] which rigorously found deterministic hydrodynamic equations for two, one-dimensional models of motility induced phase separation (MIPS) and flocking [38]. Comparisons of the hydrodynamic equations and lattice gas simulations then showed near perfect agreement.

These deterministic hydrodynamic equations capture the most probable behaviour, however the underlying stochasticity means that trajectories can deviate wildly from the deterministic hydrodynamics. Such rare events, or *large deviations* may also be examined, and a generalisation of the central limit theorem tells us that they are exponentially unlikely [39–42]. More precisely, these trajectories have probability

$$\mathcal{P}[\text{traj}] \asymp \exp[-\mathcal{A}/\epsilon], \quad (1)$$

where ϵ is a small parameter usually related to the lattice spacing. \mathcal{A} is the large deviation function (LDF), analogous to the standard Onsager-Machlup action in dynamic field theory [28, 43–49]. Importantly, the LDF not only contains information about individual trajectories, but may be used to calculate the *stationary* probability distribution [50].

In this paper we use these methods to take the two lattice models of active matter introduced in Ref. [37] and connect them with other, more standard hydrodynamic theories of active matter [3]. For instance, the standard field theory of MIPS, active model B+ [15] is written in terms of a single field, the density. In contrast, the lattice gas hydrodynamics uses two, the density and magnetisation. To connect the two we take inspiration from standard gradient expansions [20, 51], and apply a weakly non-linear analysis near the critical point. Doing this, we show that the two theories can be

mapped onto each other exactly near the MIPS critical point. In fact, we show that the dynamics become perfectly equilibrium-like at the critical point, with non-equilibrium terms emerging as one leaves the critical region. Initially doing this on the deterministic hydrodynamics, we later include fluctuations using the LDF. This allows us to show that the near critical stationary probability distribution is the exponential of a ϕ^4 free energy. We then perform similar calculations for the hydrodynamics of the flocking model, and a new model of MIPS based on quorum sensing, finding analogous results.

The rest of the paper is structured as follows: in Sec. 2 we introduce lattice gases, the field theoretic framework, and show how to take proper hydrodynamic limits. In Sec. 3 we study the first model of MIPS, re-deriving the known LDF and analysing its near critical behaviour. We then repeat the same calculation for a model of flocking and a second model of MIPS in Secs. 4 and 5 yielding very similar results. Our results are then discussed in Sec. 6. Note that in the first two sections we have aimed for pedagogy and included more detail, whereas the last sections focus on results.

2. Lattice gases and Path integrals

Here we introduce stochastic lattice gases and show how to derive their hydrodynamic large deviation functions using path integrals.

As sketched in Fig. 1, the state of a stochastic lattice gas is given by a configuration of particles, \mathcal{C} , sitting on the discrete sites of a lattice. Dynamics are introduced by letting particles move around or chemically react, changing the configuration to \mathcal{C}' at rate $\mathcal{W}(\mathcal{C} \rightarrow \mathcal{C}')$ [26, 27, 52, 53]. This evolution is stochastic, and using these rates, the probability of seeing a given configuration, $\mathcal{P}(\mathcal{C})$, follows the master equation [54, 55]

$$\partial_t \mathcal{P}(\mathcal{C}) = \sum_{\mathcal{C}'} \mathcal{W}(\mathcal{C}' \rightarrow \mathcal{C}) \mathcal{P}(\mathcal{C}') - \mathcal{W}(\mathcal{C} \rightarrow \mathcal{C}') \mathcal{P}(\mathcal{C}). \quad (2)$$

For example, the master equation describing a box of n particles which may react to produce Δn more at rate $r(n)$ is

$$\partial_t \mathcal{P}(n) = r(n - \Delta n) \mathcal{P}(n - \Delta n) - r(n) \mathcal{P}(n). \quad (3)$$

Our initial goal is to generalise this master equation from one box, to a full lattice. For this, it is helpful to expose the linearity of the master equation by re-writing the equation in operator form

$$\partial_t \mathcal{P}(n) = \mathcal{H} \mathcal{P}, \quad \mathcal{H} = (e^{-\Delta n \partial_n} - 1) r(n), \quad (4)$$

where we used the identity $e^{\partial_n} f(n) = f(n+1)$. The evolution operator, or Hamiltonian, \mathcal{H} , is a product of two terms: the rate $r(n)$, and an exponential minus one, which controls the particle production. This structure is generic, and can be extended to act on a lattice gas by defining an occupation number n_i for each lattice site i :

$$\mathcal{H}(\partial_{n_i}, n_i) = \sum_i (e^{-\Sigma_i \Delta n_i \partial_{n_i}} - 1) r(\{n_i\}), \quad (5)$$

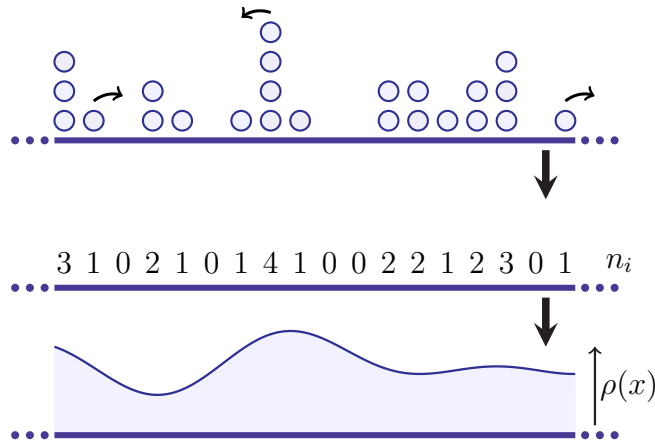


Figure 1: Schematic of a one dimensional, periodic lattice gas and its hydrodynamic description. The top line represents a single configuration of particles, with the arrows denoting some possible hops. In the second line we have converted to occupation numbers, n_i . In the final line we show the smooth density that arises through coarse graining the occupation numbers.

where the rate $r(\{n_i\})$ may depend on the occupations of all sites. Multiple species of particle can also be accommodated through an additional occupation number n^α for each species α .

For complicated lattice gas dynamics, these Hamiltonians are much easier to write down than the full master equation. To see this, consider the one dimensional lattice gas shown in Fig. 1, where the only process is diffusion. We model this as particles hopping symmetrically at rate 1 onto neighbouring sites, with no limit on the number of particles per site. Using the general Hamiltonian of Eq. (5) we write the Hamiltonian as the sum of two hopping terms, one which moves a particle to the neighbouring right site, and the other which takes a particle to the left

$$\mathcal{H} = \sum_i (e^{-\partial_{n_{i+1}} + \partial_{n_i}} - 1) n_i + (e^{-\partial_{n_{i-1}} + \partial_{n_i}} - 1) n_i. \quad (6)$$

With a little cleverness, the jump rates \mathcal{W} can be cooked up to model almost any process, and we recommend Refs. [18, 52, 56] for other interesting examples.

2.1. Path integral

With lattice gases introduced, we would now like to derive hydrodynamic equations and LDFs describing their macroscopic behaviour. Although not necessary, it is easiest to first cast the master equation as a path integral because it naturally gives the trajectory probabilities. There are various path integral representations of master equations, perhaps most famous being that of Doi and Peliti [18, 56–58], which works by converting the master equation to second quantised form and using coherent states. Not only is this algebraically cumbersome, it can be difficult to map Doi-Peliti variables to physical

particle densities [59]. As such, we instead use a more direct method [60, 61], similar to the approach introduced in Refs. [62, 63].

The key object of interest is the evolution operator taking the probability at time zero to the probability at time T , and similar to quantum mechanics, this is given by the exponential of the Hamiltonian, $\exp[\mathcal{H}T]$. As we show in [Appendix A](#), this has the path integral representation

$$\int \mathcal{D}[n_i, \hat{n}_i] \exp \left[- \int_0^T dt \left(\sum_i \hat{n}_i \partial_t n_i \right) - \mathcal{H}(\hat{n}_i, n_i) \right], \quad (7)$$

where \hat{n} is the conjugate ‘momentum’, taking the place of $-\partial_n$ in the Hamiltonian. In this representation, the general form of the Hamiltonian is even clearer, with

$$\mathcal{H}(n_i, \hat{n}_i) = \sum_i (e^{\sum_i \Delta n_i \hat{n}_i} - 1) r(\{n_i\}). \quad (8)$$

To derive hydrodynamic equations from this we now coarse grain the microscopic particle numbers n_i , into a smooth density field $\rho(x)$ [26, 46].

2.2. Hydrodynamic limit

In performing this smoothing, one may be tempted to directly replace n_i with $\rho(x)$ everywhere. However, such a mean-field approximation generally fails, and gives incorrect hydrodynamic equations [36, 59]. To remedy this, we must be more careful and use the notion of local equilibrium [26, 27, 63].

To do this we first write the Hamiltonian as the sum of a Hamiltonian density, $\mathcal{H} = \sum_i H(\{n_i, \hat{n}_i\})$. We then divide the lattice up into mesoscopic boxes of linear dimension δ centred on the lattice sites, where δ is much larger than the lattice spacing, ϵ , but much smaller than the system size [46]. Using this, we then re-write the Hamiltonian as a sum over boxes

$$\mathcal{H} = \sum_x \frac{1}{|B_\delta(x)|} \sum_{i \in B_\delta(x)} H(\{\hat{n}_i, n_i\}). \quad (9)$$

where $|B_\delta(x)|$ is the number of sites in the box and must be included to avoid over counting.

Local equilibrium then assumes that each of these boxes rapidly relaxes to a local equilibrium state that is near constant in each box, but which evolves slowly over the macroscopic, hydrodynamic scale [31, 46, 64]. The average number of each particles in each box is then equal to the slowly varying density $\rho(x, t)$, and the empirical averages over each box are assumed to converge to the average over the (as yet unknown) local equilibrium measure. Mathematically this means

$$\frac{1}{|B_\delta(x)|} \sum_{i \in B_\delta(x)} H(\{\hat{n}_i, n_i\}) \rightarrow \langle H(\{\hat{n}_i, n_i\}) \rangle, \quad (10)$$

where the angle brackets mean an average over local equilibrium. Here it is an assumption, however for the first two models we study this local equilibrium structure has been rigorously established [37, 38].

Using that this density varies slowly over the lattice, we exchange the sum over sites with an integral, yielding

$$\mathcal{H}(\hat{\rho}, \rho) = \epsilon^{-d} \int d\mathbf{r} \langle H(\{\hat{n}_i, n_i\}) \rangle, \quad (11)$$

where we have also relabelled \hat{n} to $\hat{\rho}$, and used d for the spatial dimension. In general we must also perform some extra steps like Taylor expanding the fields around each site, but this is better seen through example.

Substituting these results into (7) yields the hydrodynamic path integral governing the stochastic evolution of the density field ρ

$$\begin{aligned} \mathcal{P}[\rho(\mathbf{r}, t)] &= \int \mathcal{D}[\rho, \hat{\rho}] e^{-\mathcal{A}/\epsilon^d}, \\ \mathcal{A} &= \int dt \int d\mathbf{r} \hat{\rho} \partial_t \rho - \mathcal{H}(\hat{\rho}, \rho). \end{aligned} \quad (12)$$

The factor of ϵ^{-d} in the exponent means that the probability of observing a single trajectory takes large deviation form, $\mathcal{P} \asymp \exp[-\mathcal{A}/\epsilon^d]$, and so we identify the action \mathcal{A} as the LDF for a single trajectory.

2.3. Hydrodynamics for diffusion

Our discussion thus far has been rather formal, so we now demonstrate the approach using the one dimensional diffusion model introduced earlier. Using the conjugate variable, the Hamiltonian in Eq. (6) is re-written as

$$\mathcal{H} = \sum_i (e^{\hat{n}_{i+1} - \hat{n}_i} + e^{\hat{n}_i - \hat{n}_{i+1}} - 2) n_i. \quad (13)$$

We then have to take the average over local equilibrium. Because this Hamiltonian is linear in the occupation number, n_i , it turns out we do not need to know the exact equilibrium measure as $\langle n_i \rangle = \rho(x)$ by definition. However, as we need a similar result later, let us note that the local equilibrium measure is known to be product Poissonian [49], i.e.

$$\mu_{\text{eqm}} = \prod_i \frac{\rho_i^{n_i} e^{-\rho_i}}{n_i!}. \quad (14)$$

This follows quite naturally from the fact that we can have an arbitrary number of particles per site, and that they are non-interacting. Performing the average over \mathcal{H} we arrive at the same expression with n swapped for ρ . Assuming the density is smooth we then exchange the sum for an integral and Taylor expand the fields to $O(\epsilon)$ about each site, yielding

$$\mathcal{H} = \epsilon \int d\mathbf{r} \rho \partial_x^2 \hat{\rho} + \rho (\partial_x \hat{\rho})^2 + O(\epsilon^2). \quad (15)$$

Substituting this Hamiltonian into the action, the final (optional) steps are to diffusively re-scale time according to $dt \rightarrow \epsilon^{-2}dt$ and perform some integrations by parts. Doing this we arrive at the known LDF for non-interacting diffusing particles [46]

$$\mathcal{A} = \int d\mathbf{r} \int dt \hat{\rho}(\partial_t \rho - \partial_x^2 \rho) - \rho(\partial_x \hat{\rho})^2. \quad (16)$$

Because this LDF is quadratic in $\hat{\rho}$, hydrodynamic equations can be extracted by noting that this LDF is equivalent to the Martin–Siggia–Rose–Janssen–De Dominicis (MSRJD) action [65–67] for the noisy diffusion equation

$$\partial_t \rho = \partial_x^2 \rho + \partial_x \xi, \quad (17)$$

where ξ is a Gaussian noise with variance

$$\langle \xi(x, t) \xi(x', t') \rangle = 2\epsilon \rho \delta(x - x') \delta(t - t'). \quad (18)$$

The scaling of the noise with the lattice spacing means that the deterministic hydrodynamic equations become exact in the limit of zero lattice spacing.

With the framework laid out we turn to the main focus of the text, active lattice gases.

3. Motility induced phase separation

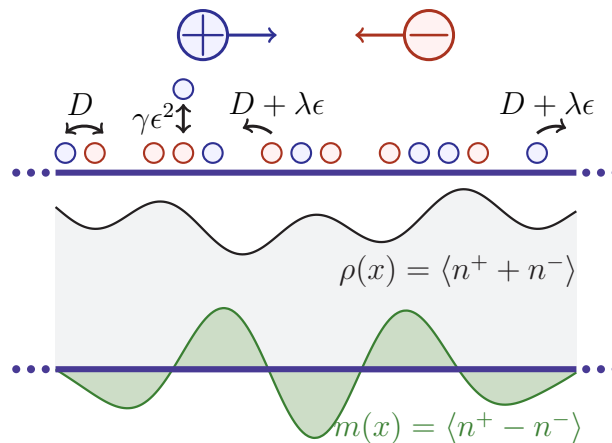


Figure 2: Schematic of the MIPS model. Blue particles are positive and propel right, red particles are negative and propel left, and there is only one particle allowed per site. The first line shows the possible microscopic moves. The second line shows the hydrodynamic fields, the grey region gives the total density ρ , and the green the magnetisation m .

In this section we study the hydrodynamic behaviour of a lattice model of MIPS first introduced in Ref. [37]. Similar to other run and tumble systems [6], we have two species of self-propelling particle n^\pm , each with a preferred direction of propulsion; while

hard core interactions are ensured by only allowing one particle per site. The microscopic dynamics include diffusion, where two neighbouring lattice sites swap occupants at rate D ; self propulsion where plus (minus) particles hop right (left) onto empty sites at rate $\lambda\epsilon$; and ‘tumbling’ where particles turn around by switching type at rate $\gamma\epsilon^2$. A schematic of these rules are shown in Fig. 2. Simulations of this system show that at sufficiently high self propulsion and density, the system undergoes MIPS and phase separates into a dense and dilute phase [37].

To construct the hydrodynamic theory we start with the Hamiltonian, written down using the above rates and Eq. (8). The result is

$$\begin{aligned} \mathcal{H} = & \sum_{|i-j|=\epsilon} \sum_{\alpha=\pm} D n_i^\alpha (1 - n_j) (e^{\hat{n}_j^\alpha - \hat{n}_i^\alpha} - 1) + D n_i^\alpha n_j^{-\alpha} (e^{\hat{n}_j^\alpha - \hat{n}_i^\alpha - \hat{n}_j^{-\alpha} + \hat{n}_i^{-\alpha}} - 1) \\ & + \lambda \epsilon n_i^\alpha (1 - n_{i+\alpha}) (e^{\hat{n}_{i+\alpha}^\alpha - \hat{n}_i^\alpha} - 1) + \gamma \epsilon^2 n_i^\alpha (e^{\hat{n}_i^{-\alpha} - \hat{n}_i^\alpha} - 1), \end{aligned} \quad (19)$$

where we have defined the total number of particles on a site as $n_i = n_i^+ + n_i^-$. The terms proportional to D govern symmetric diffusion, to λ govern self propulsion, and to γ swap the species of each particle. Although we have written the Hamiltonian concisely as a sum over species, when constructing it we find it easier to explicitly write down the terms for the plus and minus particles separately.

To derive the LDF from this Hamiltonian we need to know the local equilibrium measure. This is found by observing that the scaling of the propulsion and tumble rates with ϵ is a trick to ensure that all processes happen on a diffusive time scale. As such, diffusion occurs more frequently on a microscopic scale and controls the equilibrium measure [49]. We then use that the diffusion is equivalent to two coupled simple symmetric exclusion processes [28, 49], as to a plus (minus) particle, the minus (plus) particles act just like empty sites. As proved rigorously in Ref. [38], this implies that the local equilibrium measure is a product of Bernoulli distributions over each site for each species.

$$\mu_{\text{eqm}} = \prod_{i,\alpha} \rho_i^\alpha n_i^\alpha + (1 - \rho_i^\alpha)(1 - n_i^\alpha). \quad (20)$$

With the equilibrium measures established we now follow the steps of Sec. 2 to derive the hydrodynamic LDF. The algebra turns out to be extremely tedious and so we leave the full details to Appendix D. To summarise the process: we first average over the equilibrium measures, then Taylor expand to leading order in ϵ , before diffusively rescaling time: $dt \rightarrow \epsilon^{-2}dt$. The result is simplified by changing to density and magnetisation variables: $\rho = \rho^+ + \rho^-$, $m = \rho^+ - \rho^-$, $\hat{\rho}^+ = (\hat{\rho} + \hat{m})$, $\hat{\rho}^- = (\hat{\rho} - \hat{m})$. The density ρ gives the average number of particles per site, whereas the magnetisation, m , measures the average alignment of all the particles. Substitution of these definitions

yields

$$\begin{aligned}
 \mathcal{A} = & \int d\mathbf{r} \int dt \hat{\rho}[\partial_t \rho + \lambda \partial_x(m(1-\rho)) - D \partial_x^2 \rho] + \hat{m}[\partial_t m + \lambda \partial_x(\rho(1-\rho)) - D \partial_x^2 m] \\
 & - D \rho(1-\rho)(\partial_x \hat{\rho})^2 - D(\rho - m^2)(\partial_x \hat{m})^2 - 2Dm(1-\rho)(\partial_x \hat{\rho})(\partial_x \hat{m}) \\
 & + \gamma \rho[1 - \cosh 2\hat{m}] + \gamma m \sinh 2\hat{m},
 \end{aligned} \tag{21}$$

which is precisely the known LDF that was derived through a mapping to the ABC model [68,69]. We now use this LDF to study the critical behaviour of the hydrodynamic fields.

3.1. Deterministic behaviour

Before including fluctuations we first examine the deterministic hydrodynamic behaviour. Because this LDF is not Gaussian in the conjugate variables, we cannot directly apply the MDRJD formalism to extract the hydrodynamics equations. Instead, we note that in small lattice spacing limit the path integral may be evaluated using the saddle point method [46]. Extremising the LDF, we find the saddle point trajectories solve Hamilton's equations

$$\begin{aligned}
 \partial_t \rho &= \frac{\delta \mathcal{H}}{\delta \hat{\rho}}, & \partial_t \hat{\rho} &= -\frac{\delta \mathcal{H}}{\delta \rho}, \\
 \partial_t m &= \frac{\delta \mathcal{H}}{\delta \hat{m}}, & \partial_t \hat{m} &= -\frac{\delta \mathcal{H}}{\delta m},
 \end{aligned} \tag{22}$$

where the conjugate variables act like momenta. Although complicated, to find the deterministic hydrodynamic equations we only need the trivial solution $\hat{\rho} = \hat{m} = 0$, corresponding to noiseless, deterministic motion [18,52,70–72].

Substituting these into Hamilton's equations we arrive at a set of coupled PDEs for the fields ρ, m :

$$\begin{aligned}
 \partial_t \rho + \lambda \partial_x m(1-\rho) &= D \partial_x^2 \rho, \\
 \partial_t m + \lambda \partial_x \rho(1-\rho) &= D \partial_x^2 m - 2\gamma m,
 \end{aligned} \tag{23}$$

which are the hydrodynamic equations previously derived by more conventional methods in Ref. [37]. These can be simplified by re-scaling space-time as $x \rightarrow \sqrt{D/\gamma}x$, $t \rightarrow t/\gamma$, and defining the Péclet number $\text{Pe} = \lambda/\sqrt{D\gamma}$.

$$\begin{aligned}
 \partial_t \rho + \text{Pe} \partial_x(m(1-\rho)) &= \partial_x^2 \rho, \\
 \partial_t m + \text{Pe} \partial_x(\rho(1-\rho)) &= \partial_x^2 m - 2m.
 \end{aligned} \tag{24}$$

In Ref. [37] simulations of these PDEs and the underlying lattice gas were shown to be in excellent agreement. By performing a linear stability analysis of uniform, unmagnetised states with $\rho = \rho_0$ and $m = 0$, phase separation is predicted above the blue spinodal line in Fig. 3. This spinodal line ends at the MIPS critical point where $\rho_c = 3/4$ and $\text{Pe}_c = 4$ [37].

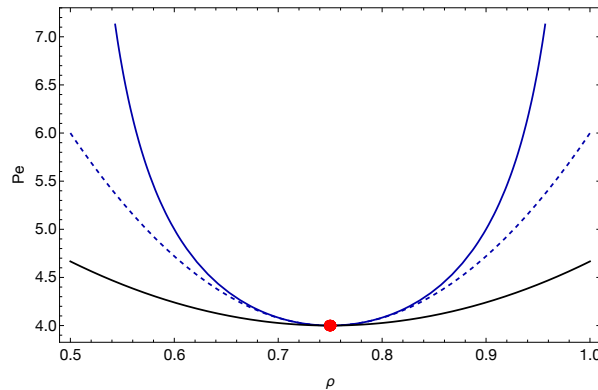


Figure 3: Phase diagram for MIPS. The blue line indicates the spinodal calculated from the hydrodynamic equations. Above this line homogeneous states are unstable and phase separate. The dashed blue line is the spinodal from the ϕ^4 free energy which agrees with the full spinodal near the critical point. The black line is the binodal from the free energy. The red dot marks the critical point where the spinodal and binodal meet.

3.2. Connection to active model B+

We have succeeded in re-deriving the hydrodynamic equations and large deviation function that were first given in Refs. [37, 68, 73]. Now we connect these to the standard field theory of MIPS, active model B+ (AMB+) [15].

AMB+ is a field theory for MIPS written in terms of a single variable ϕ , measuring the difference to the average density [3]. Although originally introduced phenomenologically, derivations from other microscopic models have shown that its predictions are most accurate near the critical point [20]. Inspired by this, we now apply a weakly non-linear analysis near the critical point to see if the lattice gas hydrodynamics can also be mapped onto AMB+ [74]. For those unfamiliar with weakly non-linear theory, it may be thought of as a formalisation of the standard Landau-Ginzburg expansion that is ordinarily performed near a critical point [18, 75].

As is standard in weakly non-linear theory, we first need a small parameter measuring the distance to the critical point [74, 76]. The natural choice here is to set $Pe = 4(1 + r)$, with r a small parameter, analogous to the reduced temperature in equilibrium [75]. The next step applies a multiple scales analysis, for which we need a set of slow space-time variables. These can be found using the linear stability analysis [77], giving $\tau = r^2 t$, and $X = r^{1/2} x$. Using these, we perform an asymptotic expansion of the density and magnetisation fields

$$\begin{aligned} \rho &= \frac{3}{4} + r^{1/2} \rho_1(X, \tau) + r \rho_2(X, \tau) + \dots, \\ m &= r^{1/2} m_1(X, \tau) + r m_2(X, \tau) + \dots \end{aligned} \tag{25}$$

These expansions are substituted into Eq. (24), before being solved order by order

in r . At leading order, we find that the magnetisation is slaved to the density, with

$$m_1 = 0, \quad m_2 = \partial_x \rho_1, \quad (26)$$

and at $O(r^{5/2})$ we get

$$\partial_\tau \rho_1 = 32\rho_1(\partial_X \rho_1)^2 - 2\partial_X^2 \rho_1 + 16\rho_1^2 \partial_X^2 \rho_1 - \frac{1}{2}\partial_X^4 \rho_1. \quad (27)$$

Converting back to the original space-time variables and letting $\phi = \rho - \rho_c$, we can put Eq. (27) in equilibrium model B form [78]

$$\partial_t \phi = \partial_x \left(\partial_x \frac{\delta \mathcal{F}}{\delta \phi} \right), \quad (28)$$

where the free energy \mathcal{F} takes ϕ^4 form

$$\mathcal{F} = \int \mathrm{d}\mathbf{r} \quad -r\phi^2 + \frac{4}{3}\phi^4 + \frac{1}{4}(\partial_x \phi)^2. \quad (29)$$

As shown in Fig. 3, the spinodals from this free energy agree with the full spinodals calculated from Eq. (24) near the critical point. This suggests that the model lies in the mean-field model B universality class when the lattice spacing tends to zero.

Of course, model B is not equivalent to AMB+, however this can be derived by continuing the calculation to next order in r . At $O(r^3)$ we find an equation that can be combined with (28) to give

$$\partial_t \phi = \partial_x \left(\partial_x \frac{\delta \mathcal{F}}{\delta \phi} - 6(\partial_x \phi) \partial_x^2 \phi \right), \quad (30)$$

which is exactly AMB+. This is satisfying as active model B+ is normally derived non-rigorously, whereas here it *exactly* captures the dynamics near the critical point.

3.3. Transition probabilities and stationary distribution

The analysis above suggests that the probability of seeing a fluctuation might be given by the exponential of a free energy difference as in equilibrium [12, 79]. To check this we must calculate the probability of transitioning between two states, i.e. we must perform the path integral over the fields conditioned on the initial and final states. As in the deterministic case, the path integral will be dominated by the saddle points; the difference here being that $\hat{\rho}, \hat{m}$ will not be zero as we need to consider fluctuations. As a starting state we choose a fixed point of the dynamics [28], which must be noise-less with $\hat{\rho} = \hat{m} = 0$. The Hamiltonian dynamics then implies that the Hamiltonian is zero for all time, giving the transition probability as

$$\mathcal{P}[\text{transition}] \asymp \exp \left[-\epsilon^{-1} \int_0^T dt \int \mathrm{d}\mathbf{r} \quad \hat{\rho} \partial_t \rho + \hat{m} \partial_t m \right], \quad (31)$$

where $\hat{\rho}, \hat{m}$ are evaluated along the extremal path.

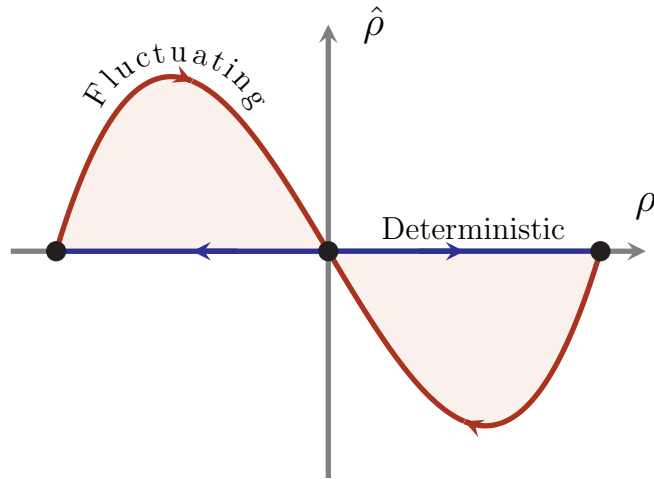


Figure 4: Schematic zero Hamiltonian trajectories just above the critical point with $r > 0$. The thick black dots mark the fixed points, which are all noiseless with $\hat{\rho} = 0$. The central point is the homogeneous state with $\rho = \rho_c$, and the points either side are the phase separated densities. The fluctuating trajectories that increase the free energy are red, and have $\hat{\rho} \neq 0$. The blue lines that decrease the free energy are deterministic, with $\hat{\rho} = 0$. The area of the shaded region gives the action required to transition between each fixed point, which for a system in equilibrium is equivalent to the free energy difference.

Although we are not able to solve Eq. (22) exactly, we can solve them perturbatively. Again, we do this with weakly non-linear theory, and the result is that all variables are slaved to the density,

$$\hat{\rho} = \frac{16\sqrt{D}}{3\sqrt{\gamma}} \frac{\delta\mathcal{F}}{\delta\phi} + O(r^2), \quad \hat{m} = O(r^2). \quad (32)$$

Substituting these into the transition probability and integrating with respect to time gives us the standard Kramers result from equilibrium statistical mechanics

$$\mathcal{P}[\text{transition}] \asymp \exp\left[-\frac{16\sqrt{D}}{3\epsilon\sqrt{\gamma}} \Delta\mathcal{F}\right], \quad (33)$$

where $\Delta\mathcal{F}$ is the change in free energy between the initial and final state.

Importantly, this calculation only holds if the final state has a larger free energy than the initial state; and as shown in Fig. 4, this is because the fluctuating trajectories that leave the fixed points always serve to increase the free energy. In contrast, the trajectories that decrease the free energy are always deterministic with $\hat{\rho} = \hat{m} = 0$ [80,81]. Using these results and large deviation theory [50], it follows that the probability distribution for ϕ is equilibrium-like near the critical point, i.e.

$$\mathcal{P}[\phi(x)] \asymp \exp\left[-\frac{16\sqrt{D}}{3\sqrt{\gamma}\epsilon} \mathcal{F}\right]. \quad (34)$$

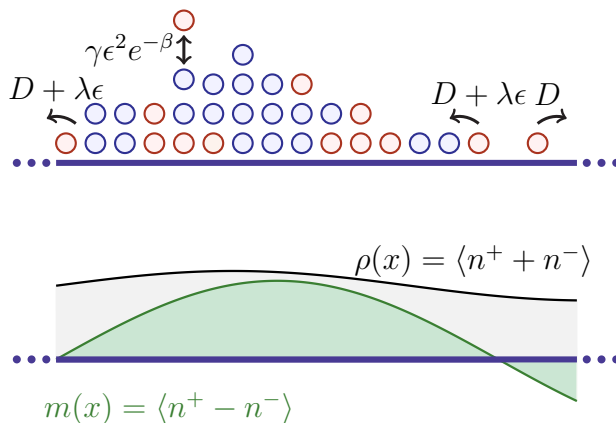


Figure 5: Schematic of the flocking model. Multiple particles are allowed per site, and particles change species at a rate that depends on the local magnetisation. Blue particles are positive, red particles are negative. The first line gives the allowed microscopic moves. The second line shows the hydrodynamic fields, the gray gives the total density, and the green the magnetisation.

Unfortunately we do not find it possible to calculate any higher order corrections to this as the AMB+ terms are non integrable [82]. Eqs. (30) and (34) are key results of the paper, and in the next section we perform similar calculations for two other models.

4. Flocking

Our second active lattice gas is the one dimensional flocking model introduced in [37], although similar to other lattice flocking models [35, 36]. This model is designed to mimic the Vicsek mechanism for the transition to collective motion [9].

As in MIPS, we have two species of particle n^\pm on a one dimensional lattice, but there is no limit to the number of particles on each site. Diffusion and self propulsion comes from plus (minus) particles hopping right (left) at rate $D + \lambda\epsilon$, and hopping left (right) at rate D . Flocking is induced through a Glauber type term, with n^\pm particles switching type at rate $\gamma\epsilon^2 \exp[\mp\beta(n^+ - n^-)]$. See Fig. 5 for a schematic.

As before, the Hamiltonian is written down using the general rules, giving

$$\begin{aligned} \mathcal{H} = & \sum_i \sum_{\alpha=\pm} D n_i^\alpha (e^{\hat{n}_{i+1}^\alpha - \hat{n}_i^\alpha} + e^{\hat{n}_{i-1}^\alpha - \hat{n}_i^\alpha} - 2) + \lambda\epsilon n_i^\alpha (e^{\hat{n}_{i+\alpha}^\alpha - \hat{n}_i^\alpha} - 1) \\ & + \gamma\epsilon^2 n_i^\alpha e^{-\alpha\beta(n_i^+ - n_i^-)} (e^{\hat{n}_i^{-\alpha} - \hat{n}_i^\alpha} - 1). \end{aligned} \quad (35)$$

where the first term gives diffusion, the second self propulsion, and the the last gives flocking.

Again, the rates are chosen such that diffusion dominates locally and controls the local equilibrium. Unlike MIPS, but as in the earlier diffusion model, there is no limit to the number of particles per site. This implies that the local equilibrium measure is a

product of Poisson rather than Bernoulli measures over each site and each species [37]. Performing the average over local equilibrium and Taylor expanding, we find

$$\begin{aligned}
 \mathcal{A} = & \int d\mathbf{r} \int dt \hat{\rho}[\partial_t \rho + \lambda \partial_x m - D \partial_x^2 \rho] + \hat{m}[\partial_t m + \lambda \partial_x \rho - D \partial_x^2 m] \\
 & - D \rho (\partial_x \hat{\rho})^2 - D \rho (\partial_x \hat{m})^2 - 2Dm (\partial_x \bar{\rho}) (\partial_x \hat{m}) - \\
 & \frac{\gamma e^{-\beta}}{2} (\rho + m) \exp[\rho (\cosh \beta - 1) - m \sinh \beta] (e^{-2\hat{m}} - 1) \\
 & - \frac{\gamma e^{-\beta}}{2} (\rho - m) \exp[\rho (\cosh \beta - 1) + m \sinh \beta] (e^{2\hat{m}} - 1),
 \end{aligned} \tag{36}$$

where, as before, we have changed to density and magnetisation variables. This LDF was previously found using Doi-Peliti theory [83], although it wasn't recognised as a large deviation function. The results are the same because coherent states used in Doi-Peliti are equivalent to Poisson distributions [18, 52, 56, 83, 84]. Using other lattice gases, we have checked that this method reproduces the results of Doi-Peliti theory but have not been able to prove an exact equivalence. We believe this approach to be simpler than Doi-Peliti because the Hamiltonian need not be converted into creation and annihilation operators.

4.1. Deterministic behaviour

The deterministic equations from this action agree with those derived in [37], and are given by

$$\begin{aligned}
 \partial_t \rho + \text{Pe} \partial_x m &= \partial_x^2 \rho, \\
 \partial_t m + \text{Pe} \partial_x \rho &= \partial_x^2 m - 2F(\rho, m), \\
 F(\rho, m) &= (m \cosh[m \sinh(\beta)] - \rho \sinh[m \sinh(\beta)]) \\
 &\quad \times e^{-\beta + \rho \cosh(\beta) - \rho},
 \end{aligned} \tag{37}$$

where we have performed the same re-scaling of space and time as earlier. If all the particles align the system is said to be flocking, with m homogeneous and non-zero. This can happen even at zero self propulsion ($\text{Pe} = 0$), and homogeneous states $\rho = \rho_0, m = 0$ are unstable to flocks when $\rho_0 > (\sinh \beta)^{-1}$.

To understand this transition we again perform a weakly non-linear analysis, letting $\beta = \text{arcsinh}(1/\rho_0)(1+r)$, and $X = r^{1/2}x, \tau = rt$. Note that the slow time scale scales like r rather than r^2 as the magnetisation is not a conserved quantity [76].

Expanding the fields as in Eq. (25), we find that we must work to $O(r^2)$ to get a consistent set of equations. The details of the calculation are left to Appendix E, but the result is that near the instability

$$\begin{aligned}
 \partial_t \phi &= \partial_x^2 \phi, \\
 \partial_t m &= \partial_x^2 m + Arm + 6B\rho_0 m \phi - 2Bm^3, \\
 A &= 6B\rho_0 \sqrt{1 + \rho_0^2} \text{arcsinh}(1/\rho_0), \\
 B &= \frac{1}{3\rho_0^2} \exp\left[-\rho_0 + \sqrt{1 + \rho_0^2} - \text{arcsinh}(1/\rho_0)\right],
 \end{aligned} \tag{38}$$

where $\phi = \rho - \rho_c$. These equations do not derive from a single free energy, and so initially one may think that the dynamics are not in an equilibrium class. However, the density perturbation is decoupled from the magnetisation and diffusively relaxes, while the magnetisation is still critically slowed. Therefore over long times we may assume that the density perturbation relaxes to zero. Substituting this into the magnetisation equation we find the dynamics of m take model A form, with

$$\partial_t m = -\frac{\delta \mathcal{F}}{\delta m}, \quad (39)$$

and a free energy

$$\mathcal{F} = \int d\mathbf{r} \left[-\frac{Ar}{2}m^2 + \frac{B}{2}m^4 + \frac{1}{2}(\partial_x m)^2 \right]. \quad (40)$$

In other words, the free energy is still Ising type over long time scales, however the order parameter, m , is not conserved. These conclusions agree with the numerical simulations of similar, two dimensional lattice flocking models which showed that the critical dynamics at zero Péclet number were in the Ising universality class [35, 36].

4.2. Stationary distribution

The stationary distribution can be calculated in much the same way as for MIPS. Assuming that the density has already relaxed to a uniform value, we find the near critical magnetisation distribution to be Boltzmannian

$$\mathcal{P}(m) \asymp \exp \left[-\frac{4\rho_0\sqrt{D}}{4B\sqrt{\gamma\epsilon}} \mathcal{F} \right]. \quad (41)$$

5. Quorum sensing MIPS

We now turn to an alternative model of MIPS to argue that our conclusions about Ising universality are not model dependent. Rather than enforcing a hard-core constraint between particles as in section 3, we induce the MIPS transition through quorum sensing. Quorum sensing allows multiple particles per site, but decreases the self propulsion speed at regions of high density [5, 6]. To put this on a lattice we use a near identical set up to the earlier MIPS model with two types of particle, but change the self propulsion rate to $\epsilon\lambda_0 e^{-\sigma_0(n^++n^-)}$ to slow down particles when the density is high, see Fig. 6. As in the flocking model, the slowing down of the self-propulsion and tumbling with factors of ϵ implies that the local equilibrium measure is product Poissonian for each species at each site.

Following earlier methods we derive the coarse-grained LDF

$$\begin{aligned} \mathcal{A} = & \int d\mathbf{r} \int dt \left[\hat{\rho}[\partial_t \rho + \lambda \partial_x m e^{-\sigma\rho} - D\partial_x^2 \rho] + \hat{m}[\partial_t m + \lambda \partial_x \rho e^{-\sigma\rho} \right. \\ & - D\partial_x^2 m] - D\rho(\partial_x \hat{\rho})^2 - D\rho(\partial_x \hat{m})^2 - 2Dm(\partial_x \hat{\rho})(\partial_x \hat{m}) \\ & \left. + \gamma\rho[1 - \cosh 2\hat{m}] + \gamma m \sinh 2\hat{m}, \right] \end{aligned} \quad (42)$$

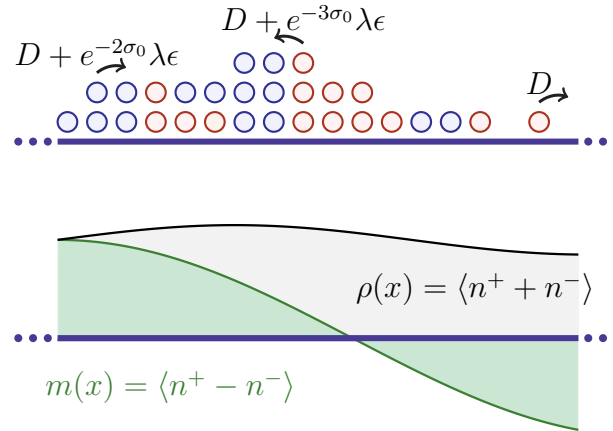


Figure 6: Schematic of the quorum sensing MIPS model. Multiple particles are allowed per site, but the self propulsion is exponentially slower at regions of high density. Blue particles are positive, red particles are negative. The first line shows the microscopic moves. The second line shows the hydrodynamic fields, the grey region gives the total density, and the green the magnetisation.

where we see that the average over local equilibrium has renormalised the self propulsion to $\lambda = \lambda_0 e^{-\sigma}$, and σ_0 to $\sigma = 1 - e^{-\sigma_0}$.

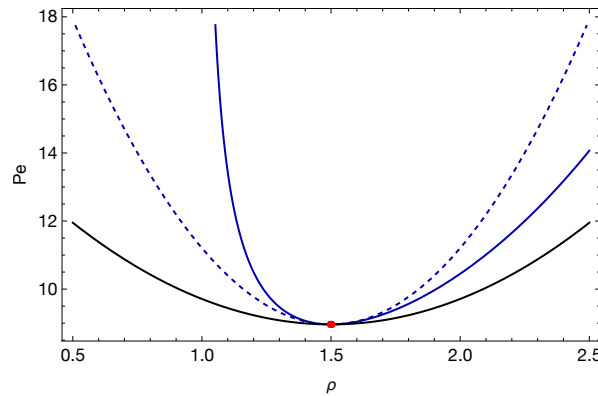


Figure 7: Phase diagram for quorum sensing MIPS. The blue line indicates the spinodal calculated from the hydrodynamic equations. Above this line homogeneous states are unstable and phase separate. The dashed blue line is the spinodal from the free energy which agrees with the full spinodal near the critical point. The black line is the binodal from the free energy. The red dot marks the critical point where the spinodal and binodal meet. Note that the full spinodal is quite asymmetric whereas the free energy spinodal is necessarily symmetric.

5.1. Critical behaviour

At deterministic level, the hydrodynamic equations are

$$\partial_t \rho + \text{Pe} \partial_x (m e^{-\rho}) = \partial_x^2 \rho, \quad (43a)$$

$$\partial_t m + \text{Pe} \partial_x (\rho e^{-\rho}) = \partial_x^2 m - 2m, \quad (43b)$$

where Pe is as defined before and we have set absorbed σ by re-scaling the density and magnetisation fields. A linear instability analysis shows that the system phase separates above the blue spinodal in Fig. 7, with the MIPS critical point at $\text{Pe}_c = 2e^{3/2}$, $\rho_c = 3/2$.

As in the previous two sections, we perform a weakly non-linear analysis near this point, finding a model B equation, with free energy

$$\mathcal{F} = \int d\mathbf{r} \quad -r\phi^2 + \frac{1}{6}\phi^4 + \frac{1}{4}(\partial_x \phi)^2, \quad (44)$$

where, again, $\phi = \rho - \rho_c$. As in Sec. 3, this shows that the phase separation in this model is equilibrium type even though the underlying dynamics are not. A phase diagram comparing the full equations and the free energy is shown in Fig. 7.

The fluctuations and stationary distribution follow similarly, and we have

$$\mathcal{P} \asymp \exp \left[-\frac{2\sqrt{D}}{9\sigma\sqrt{\gamma\epsilon}} \mathcal{F} \right]. \quad (45)$$

These results suggest, but by no means prove, that any one dimensional diffusive lattice gas undergoing the MIPS transition has near critical dynamics that live in the model B universality class.

6. Discussion

Starting from the master equations describing the stochastic dynamics we have derived hydrodynamic equations, and the corresponding large deviation functions describing the coarse grained behaviour of three active lattice gases. Using this hydrodynamic description we located their critical points and performed a series of weakly non-linear calculations, using them to argue that all the models lay in kinetic Ising universality classes, model B for MIPS, and model A for flocking [78].

These calculations were first done on the deterministic hydrodynamic equations, but were extended to include fluctuations by perturbatively solving the full saddle-point equations near the critical point. Doing this we found that the stationary probability distributions were given by the negative exponential of a free energy, just as in equilibrium, meaning that detailed balance is effectively restored asymptotically close to the critical point.

In the case of MIPS we also continued the expansion to higher order, showing that the two-field hydrodynamics reduced to active model B+, the standard field theory of motility induced phase separation [3, 15], as we left the critical region. This implies

that non-equilibrium effects do become important as one departs from the critical point, however they are irrelevant at criticality. This agrees with a number of numerical studies on the MIPS critical point, of which most conclude that it is in the Ising universality class [85–88].

In this work we focused on one dimensional systems, but the methods used here could also be used in higher dimensional systems. Unfortunately, the LDFs become extremely cumbersome, as a new species must be introduced for every lattice direction. However, it is certainly worth investigating this further, as numerical studies of two dimensional lattice models of MIPS have found some possible differences between models on square and triangular lattices [85, 88]. Moreover, the AMB+ terms become more interesting in dimensions two or higher, with there being two independent non-equilibrium terms in the density current, rather than the one in one dimension [15]. It would also be interesting to make these lattice gases thermodynamically consistent by explicitly accounting for the chemical fuel used in self-propulsion [89, 90], which would give insight into the earlier phenomenological approaches which started with the continuum equations [89]. We leave all this for future work.

Acknowledgments

We thank Tal Agranov and Tomohiro Sasamoto for helpful discussions, and Tanniemola Liverpool for a careful reading of the manuscript. This work was supported by an EPSRC studentship.

Appendices

Appendix A. Path integral derivation

The path integral representation is derived here for single species on one site, but the derivation is identical for multiple sites. To put the master equation in path integral form we use linearity to evolve the probability forwards by a small amount of time δt , $\mathcal{P}_n(\delta t) = \exp[\mathcal{H}\delta t]\mathcal{P}_n(0)$.

$$\begin{aligned}
 e^{\mathcal{H}\delta t} &\approx (1 + \mathcal{H}\delta t) \\
 &= (1 + \delta t(e^{-\Delta n \partial_n} - 1))r(n) \\
 &= \sum_{n_0} (1 + \delta t(e^{-\Delta n_0 \partial_n} - 1))\delta_{n,n_0}r(n_0) \\
 &= \int_{-i\pi}^{i\pi} \frac{d\hat{n}_0}{2\pi i} (1 + \delta t(e^{-\Delta n_0 \partial_n} - 1))e^{-\hat{n}_0(n-n_0)}r(n_0) \\
 &= \int_{-i\pi}^{i\pi} \frac{d\hat{n}_0}{2\pi i} (1 + \delta t(e^{\Delta n_0 \hat{n}_0} - 1))e^{-\hat{n}_0(n-n_0)}r(n_0) \\
 &\approx \int_{-i\pi}^{i\pi} \frac{d\hat{n}_0}{2\pi i} \exp[-\hat{n}_0(n-n_0) + \delta t(e^{\hat{n}_0 \Delta n} - 1)r(n_0)],
 \end{aligned}$$

where in the last line we have re-exponentiated the result, which is correct to $O(\delta t)$ [91]. By combining many of these evolutions we get the probability at a time T

$$\mathcal{P}_n(T) = \int \mathcal{D}[n, \hat{n}] e^{-\mathcal{S}} \mathcal{P}_n(0), \quad (\text{A.1a})$$

$$\mathcal{S} = \sum_{t=0}^{t=T-\delta t} \hat{n}_t (n_{t+\delta t} - n_t) - \delta t (e^{\Delta n \hat{n}_t} - 1) r(n_t), \quad (\text{A.1b})$$

$$\int \mathcal{D}[n, \hat{n}] = \lim_{\delta t \rightarrow 0} \prod_{t=0}^{T-\delta t} \sum_{n(t)=0}^{N_{max}} \int_{-i\pi}^{i\pi} \frac{d\hat{n}(t)}{2\pi i}. \quad (\text{A.1c})$$

It is tempting to take the continuum limit and convert the forward differences to time derivatives. However, n is always an integer valued quantity and a derivative does not exist. With this fact in mind we will write the path integral in continuous notation although it should be understood in its discrete form. In continuum form, the action is

$$\mathcal{S} = \int dt \hat{n} \partial_t n - \mathcal{H}(\hat{n}, n), \quad (\text{A.2})$$

which is the standard form from classical mechanics if \hat{n} is the conjugate ‘momentum’ to n , obeying canonical commutation relations $[n, \hat{n}] = 1$. The way we have discretised time also means that the continuum Langevin equations from this integral must be interpreted in the Itô sense [92].

Using this path integral the probability of a single trajectory through configuration space is given by

$$\mathcal{P}[\text{traj}] = \int \mathcal{D}[\hat{n}] e^{-\mathcal{S}} \mathcal{P}(t=0), \quad (\text{A.3})$$

where only \hat{n} is integrated over, while the value of n is specified at each time step.

Appendix B. Local equilibrium measures

In the main text we stated the local equilibrium measures without calculation. Although these measures are well established [49], here we give a proof sketch.

Appendix B.1. Exclusion: Bernoulli

For the SSEP, the local equilibrium measure, μ , is known to be product Bernoulli

$$\mu(\{n_i\}) = \prod_i \rho_i n_i + (1 - \rho_i)(1 - n_i), \quad (\text{B.1})$$

where ρ_i is the average density at site i which varies slowly on the microscopic scale. To derive this consider a single coarse grained box and select a site k in its interior. The particle flux from site $k-1$ to k is

$$j_{k-1,k} = p_{k-1}(1)p_k(0) - p_{k-1}(0)p_k(1), \quad (\text{B.2})$$

where $p_k(n)$ is the probability of finding n particles on site k . If the box is in local equilibrium then j must vanish and so $p_{k-1} = p_k$. Using that the number of particles is restricted to be in $(0, 1)$ we find

$$p_k(n) = \rho n + (1 - \rho)(1 - n), \quad (\text{B.3})$$

with ρ the mean number of particles at site. At this point one may conclude that the local equilibrium measure is a constant density everywhere in space but this is only the steady state distribution. In general, the mean particle number will be constant in each microscopically large coarse graining box, but will vary slowly over the diffusive macroscopic scale, leading to (B.1). One may also check that the jump rates for the SSEP respect detailed balance with respect to Eq. (B.3) meaning that it is the unique stationary measure.

Appendix C. Current form of the LDF

Macroscopic fluctuation theory considers the joint fluctuations of the density ρ , conserved current j , and flux K [46], however our LDFs are written in terms of the conjugate field $\hat{\rho}$. To demonstrate how to convert between the two we use the following LDF describing diffusion combined with particle creation and destruction at rates b and d respectively

$$\mathcal{A} = \int dt \int dx \hat{\rho}[\partial_t \rho - D\partial_x^2 \rho] - D\rho(\partial_x \hat{\rho})^2 - b(e^{\hat{\rho}} - 1) - d(e^{-\hat{\rho}} - 1)\rho. \quad (\text{C.1})$$

To put this in current form we demand that the density satisfies the exact equation

$$\partial_t \rho = -\partial_x j + K, \quad (\text{C.2})$$

where ρ , j , and K are fluctuating quantities. Let us now break apart the LDF into two pieces coming from the conserved and non-conserved current. For the conserved current alone we have an

$$\mathcal{A} = \int dt \int dx \hat{\rho}[\partial_t \rho - D\partial_x^2 \rho] - D\rho(\partial_x \hat{\rho})^2. \quad (\text{C.3})$$

We now replace $\partial_t \rho$ with $-\partial_x j$ and integrate by parts, giving the result

$$\mathcal{A}_j = \int dt \int dx j \partial_x \hat{\rho} + D(\partial_x \rho)(\partial_x \hat{\rho}) - D\rho(\partial_x \hat{\rho})^2. \quad (\text{C.4})$$

We would now like to perform the path integral over $\hat{\rho}$, and this can be done exactly, giving

$$\mathcal{A}_j = \int dt \int dx \frac{(j + D\partial_x \rho)^2}{4D\rho}. \quad (\text{C.5})$$

This quantifies how the conserved current j fluctuates around its average value $-D\partial_x \rho$. We now turn to the non-conserved current, with an LDF

$$\mathcal{A} = \int dt \int dx \hat{\rho} \partial_t \rho - b(e^{\hat{\rho}} - 1) - d(e^{-\hat{\rho}} - 1)\rho. \quad (\text{C.6})$$

Following similar methods to before we replace $\partial_t \rho$ with K and perform the path integral over $\hat{\rho}$. The $\hat{\rho}$ path integral cannot be performed exactly but can be done using a saddle point method. The result is that $\hat{\rho}$ is given by

$$e^{\hat{\rho}} = \frac{K + \sqrt{K^2 + 4bd\rho}}{2b}. \quad (\text{C.7})$$

This is substituted into the LDF to give

$$\mathcal{A}_K = \int dt \int dx b + d\rho - \sqrt{K^2 + 4bd\rho} + K \log \frac{\sqrt{K^2 + 4bd\rho} + K}{2b}. \quad (\text{C.8})$$

The total probability for a given path is then

$$\mathcal{P} \simeq \delta(\partial_t \rho + \partial_x j - K) e^{-\mathcal{I}(\rho, j, K)/\epsilon} \quad (\text{C.9})$$

where the large deviation functional is

$$\mathcal{I}(\rho, j, K) = \mathcal{A}_j + \mathcal{A}_K. \quad (\text{C.10})$$

The LDF in terms of ρ and $\hat{\rho}$ can be recovered by introducing a functional representation of the delta function and extremising the action over K and j [46].

Appendix D. MIPS LDF

Here we explicitly derive the hydrodynamic action for the MIPS model. Starting with Eq. (19) we first perform the sum over α and then take the average over the local equilibrium measure to get

$$\begin{aligned} \mathcal{H} = & \sum_i D\rho_i^+ (1 - \rho_{i+1}) \left(e^{\hat{\rho}_{i+1}^+ - \hat{\rho}_i^+} - 1 \right) + D\rho_i^+ (1 - \rho_{i-1}) \left(e^{\hat{\rho}_{i-1}^+ - \hat{\rho}_i^+} - 1 \right) \\ & + D\rho_i^- (1 - \rho_{i+1}) \left(e^{\hat{\rho}_{i+1}^- - \hat{\rho}_i^-} - 1 \right) + D\rho_i^- (1 - \rho_{i-1}) \left(e^{\hat{\rho}_{i-1}^- - \hat{\rho}_i^-} - 1 \right) \\ & + D\rho_i^+ \rho_{i-1}^- \left(e^{\hat{\rho}_{i-1}^+ - \hat{\rho}_i^+ - \hat{\rho}_{i-1}^- + \hat{\rho}_i^-} - 1 \right) + D\rho_i^+ \rho_{i+1}^- \left(e^{\hat{\rho}_{i+1}^+ - \hat{\rho}_i^+ - \hat{\rho}_{i+1}^- + \hat{\rho}_i^-} - 1 \right) \\ & + \lambda \epsilon \rho_i^+ (1 - \rho_{i+1}) \left(e^{\hat{\rho}_{i+1}^+ - \hat{\rho}_i^+} - 1 \right) + \lambda \epsilon \rho_i^- (1 - \rho_{i-1}) \left(e^{\hat{\rho}_{i-1}^- - \hat{\rho}_i^-} - 1 \right) \\ & + \gamma \epsilon^2 \rho_i^+ \left(e^{\hat{\rho}_i^- - \hat{\rho}_i^+} - 1 \right) + \gamma \epsilon^2 \rho_i^- \left(e^{\hat{\rho}_i^+ - \hat{\rho}_i^-} - 1 \right). \end{aligned} \quad (\text{D.1})$$

Exchanging the sum for an integral and Taylor expanding the fields we find

$$\begin{aligned} \mathcal{H} = & \epsilon \int d\mathbf{r} (\partial_x \hat{\rho}^+)^2 \rho^+ (1 - \rho^+) + (\partial_x \hat{\rho}^-)^2 \rho^- (1 - \rho^-) - 2(\partial_x \hat{\rho}^+) (\partial_x \hat{\rho}^-) \rho^+ \rho^- \\ & - 2(\partial_x \hat{\rho}^-) (\rho^+ \partial_x \rho^- + \rho^- \partial_x \rho^+) - 2(\partial_x \hat{\rho}^+) (\partial_x \rho^+) \rho^+ + (\partial_x^2 \hat{\rho}^-) (\rho^- (\rho^-)^2 - 2\rho^+ \rho^-) \\ & + (\partial_x^2 \hat{\rho}^+) \rho^+ (1 - \rho^+) \lambda \rho^+ (1 - \rho) (\partial_x \hat{\rho}^+) - \lambda \rho^+ (1 - \rho) (\partial_x \hat{\rho}^+) + \gamma \rho^+ \left(e^{\hat{\rho}^- - \hat{\rho}^+} - 1 \right) \\ & + \gamma \rho^- \left(e^{\hat{\rho}^+ - \hat{\rho}^-} - 1 \right), \end{aligned} \quad (\text{D.2})$$

where $\rho = \rho^+ + \rho^-$. After changing to density and magnetisation variables: $\rho = \rho^+ + \rho^-$, $m = \rho^+ - \rho^-$, $\hat{\rho}^+ = (\hat{\rho} + \hat{m})$, $\hat{\rho}^- = (\hat{\rho} - \hat{m})$ and performing many integrations by parts we arrive at the LDF from the main text.

Appendix E. Weakly non-linear calculation for flocking

The deterministic equations for the flocking model with zero self propulsion in the slow scales are

$$r^{3/2}\partial_\tau\rho = r\partial_X^2\rho, \quad (\text{E.1a})$$

$$r^{3/2}\partial_\tau m = r\partial_X^2 m - 2F(\rho, m). \quad (\text{E.1b})$$

To perform a weakly non-linear analysis we expand the fields

$$\rho = \rho_0 + r^{1/2}\rho_1 + r\rho_2 + r^{3/2}\rho_3 + \dots, \quad (\text{E.2a})$$

$$m = r^{1/2}m_1 + rm_2 + r^{3/2}m_3 + \dots \quad (\text{E.2b})$$

Substituting these expansions into the equations we find $\rho_1 = 0$. At $O(r^{3/2})$ we have

$$\partial_\tau m_1 = \partial_X^2 m_1 + Am_1 - 6B\rho_0 m_1 \rho_2 - 2Bm_1^3, \quad (\text{E.3})$$

where B is defined as in the main text, and the presence of ρ_2 means we must work to higher order in r . At $O(r^2)$ we find

$$\partial_\tau \rho_2 = \partial_X^2 \rho_2, \quad (\text{E.4a})$$

$$\partial_\tau m_2 = \partial_X^2 m_2 + Am_2 - 6B\rho_0 m_2 \rho_2 - 6Bm_1^2 m_2, \quad (\text{E.4b})$$

where A is given by the value in the main text. Defining $\phi = r\rho_2$ and using the series expansion for m , the equations at $O(r^{3/2})$ and $O(r^2)$ can be combined into a single set. Restoring the original space time scales yields the equations from the main text

$$\partial_t \phi = \partial_x^2 \phi, \quad (\text{E.5a})$$

$$\partial_t m = \partial_x^2 m + Arm - 6B\rho_0 m \phi - 2Bm^3. \quad (\text{E.5b})$$

References

- [1] Sriram Ramaswamy. The mechanics and statistics of active matter. *Annu. Rev. Condens. Matter Phys.*, 1(1):323–345, 2010.
- [2] M Cristina Marchetti, Jean-François Joanny, Sriram Ramaswamy, Tanniemola B Liverpool, Jacques Prost, Madan Rao, and R Aditi Simha. Hydrodynamics of soft active matter. *Reviews of modern physics*, 85(3):1143, 2013.
- [3] Michael E Cates. Active field theories. *arXiv preprint arXiv:1904.01330*, 2019.
- [4] Gerhard Gompper, Roland G Winkler, Thomas Speck, Alexandre Solon, Cesare Nardini, Fernando Peruani, Hartmut Löwen, Ramin Golestanian, U Benjamin Kaupp, Luis Alvarez, et al. The 2020 motile active matter roadmap. *Journal of Physics: Condensed Matter*, 32(19):193001, 2020.
- [5] Michael E Cates and Julien Tailleur. Motility-induced phase separation. *Annu. Rev. Condens. Matter Phys.*, 6(1):219–244, 2015.
- [6] J Tailleur and ME Cates. Statistical mechanics of interacting run-and-tumble bacteria. *Physical review letters*, 100(21):218103, 2008.
- [7] Yaouen Fily and M Cristina Marchetti. Athermal phase separation of self-propelled particles with no alignment. *Physical review letters*, 108(23):235702, 2012.

- [8] John Toner and Yuhai Tu. Long-range order in a two-dimensional dynamical xy model: how birds fly together. *Physical review letters*, 75(23):4326, 1995.
- [9] Tamás Vicsek, András Czirók, Eshel Ben-Jacob, Inon Cohen, and Ofer Shochet. Novel type of phase transition in a system of self-driven particles. *Physical review letters*, 75(6):1226, 1995.
- [10] Joakim Stenhammar, Adriano Tiribocchi, Rosalind J Allen, Davide Marenduzzo, and Michael E Cates. Continuum theory of phase separation kinetics for active brownian particles. *Physical review letters*, 111(14):145702, 2013.
- [11] Michael E Cates and Elsen Tjhung. Theories of binary fluid mixtures: from phase-separation kinetics to active emulsions. *Journal of Fluid Mechanics*, 836:P1, 2018.
- [12] Paul M Chaikin, Tom C Lubensky, and Thomas A Witten. *Principles of condensed matter physics*, volume 10. Cambridge university press Cambridge, 1995.
- [13] Bertrand I Halperin. On the hohenberg–mermin–wagner theorem and its limitations. *Journal of Statistical Physics*, 175(3):521–529, 2019.
- [14] Paul C Martin, Olivier Parodi, and Peter S Pershan. Unified hydrodynamic theory for crystals, liquid crystals, and normal fluids. *Physical Review A*, 6(6):2401, 1972.
- [15] Elsen Tjhung, Cesare Nardini, and Michael E Cates. Cluster phases and bubbly phase separation in active fluids: reversal of the ostwald process. *Physical Review X*, 8(3):031080, 2018.
- [16] John Toner, Yuhai Tu, and Sriram Ramaswamy. Hydrodynamics and phases of flocks. *Annals of Physics*, 318(1):170–244, 2005.
- [17] Hugues Chaté. Dry aligning dilute active matter. *Annual Review of Condensed Matter Physics*, 11:189–212, 2020.
- [18] Uwe C Täuber. *Critical dynamics: a field theory approach to equilibrium and non-equilibrium scaling behavior*. Cambridge University Press, 2014.
- [19] Alexandre P Solon, Michael E Cates, and Julien Tailleur. Active brownian particles and run-and-tumble particles: A comparative study. *The European Physical Journal Special Topics*, 224(7):1231–1262, 2015.
- [20] Alexandre P Solon, Joakim Stenhammar, Michael E Cates, Yariv Kafri, and Julien Tailleur. Generalized thermodynamics of motility-induced phase separation: phase equilibria, laplace pressure, and change of ensembles. *New Journal of Physics*, 20(7):075001, 2018.
- [21] Alberto Dinelli, Jérémy O’Byrne, and Julien Tailleur. Fluctuating hydrodynamics of active particles interacting via chemotaxis and quorum sensing: static and dynamics. *arXiv preprint arXiv:2402.05072*, 2024.
- [22] Eric Bertin, Michel Droz, and Guillaume Grégoire. Hydrodynamic equations for self-propelled particles: microscopic derivation and stability analysis. *Journal of Physics A: Mathematical and Theoretical*, 42(44):445001, 2009.
- [23] Eric Bertin, Hugues Chaté, Francesco Ginelli, Shradha Mishra, Anton Peshkov, and Sriram Ramaswamy. Mesoscopic theory for fluctuating active nematics. *New journal of physics*, 15(8):085032, 2013.
- [24] Michael Te Vrugt, Jens Bickmann, and Raphael Wittkowski. How to derive a predictive field theory for active brownian particles: a step-by-step tutorial. *Journal of Physics: Condensed Matter*, 35(31):313001, 2023.
- [25] Pierre Degond and Sébastien Motsch. Continuum limit of self-driven particles with orientation interaction. *Mathematical Models and Methods in Applied Sciences*, 18(supp01):1193–1215, 2008.
- [26] Claude Kipnis and Claudio Landim. *Scaling limits of interacting particle systems*, volume 320. Springer Science & Business Media, 2013.
- [27] Herbert Spohn. *Large scale dynamics of interacting particles*. Springer Science & Business Media, 2012.
- [28] Bernard Derrida. Microscopic versus macroscopic approaches to non-equilibrium systems. *Journal of Statistical Mechanics: Theory and Experiment*, 2011(01):P01030, 2011.
- [29] Claude Kipnis, Carlo Marchioro, and Errico Presutti. Heat flow in an exactly solvable model.

- Journal of Statistical Physics*, 27:65–74, 1982.
- [30] Anna De Masi, Pablo Augusto Ferrari, and JL Lebowitz. Rigorous derivation of reaction-diffusion equations with fluctuations. *Physical review letters*, 55(19):1947, 1985.
- [31] Anna De Masi, Pablo A Ferrari, and Joel L Lebowitz. Reaction-diffusion equations for interacting particle systems. *Journal of statistical physics*, 44(3):589–644, 1986.
- [32] Claude Kipnis, Stefano Olla, and SR Srinivasa Varadhan. Hydrodynamics and large deviation for simple exclusion processes. *Communications on Pure and Applied Mathematics*, 42(2):115–137, 1989.
- [33] Bernard Derrida, Eytan Domany, and David Mukamel. An exact solution of a one-dimensional asymmetric exclusion model with open boundaries. *Journal of statistical physics*, 69:667–687, 1992.
- [34] Alasdair G Thompson, Julien Tailleur, Michael E Cates, and Richard A Blythe. Lattice models of nonequilibrium bacterial dynamics. *Journal of Statistical Mechanics: Theory and Experiment*, 2011(02):P02029, 2011.
- [35] Alexandre P Solon and Julien Tailleur. Revisiting the flocking transition using active spins. *Physical review letters*, 111(7):078101, 2013.
- [36] Alexandre P Solon and Julien Tailleur. Flocking with discrete symmetry: The two-dimensional active ising model. *Physical Review E*, 92(4):042119, 2015.
- [37] Kourbane-Houssene. Exact hydrodynamic description of active lattice gases. *Physical review letters*, 120(26):268003, 2018.
- [38] Clément Erignoux. Hydrodynamic limit for an active exclusion process. *Mémoires de la Société Mathématique de France*, 169, 2021.
- [39] Robert L Jack and Peter Sollich. Large deviations and ensembles of trajectories in stochastic models. *Progress of Theoretical Physics Supplement*, 184:304–317, 2010.
- [40] Robert L Jack. Ergodicity and large deviations in physical systems with stochastic dynamics. *The European Physical Journal B*, 93:1–22, 2020.
- [41] Hugo Touchette. The large deviation approach to statistical mechanics. *Physics Reports*, 478(1-3):1–69, 2009.
- [42] Hugo Touchette. A basic introduction to large deviations: Theory, applications, simulations. *arXiv preprint arXiv:1106.4146*, 2011.
- [43] Lorenzo Bertini, Alberto De Sole, Davide Gabrielli, Giovanni Jona-Lasinio, and Claudio Landim. Fluctuations in stationary nonequilibrium states of irreversible processes. *Physical Review Letters*, 87(4):040601, 2001.
- [44] Lorenzo Bertini, Alberto De Sole, Davide Gabrielli, Giovanni Jona-Lasinio, and Claudio Landim. Macroscopic fluctuation theory for stationary non-equilibrium states. *Journal of Statistical Physics*, 107:635–675, 2002.
- [45] L Bertini, Alberto De Sole, D Gabrielli, Giovanni Jona-Lasinio, and C233569507120473 Landim. Stochastic interacting particle systems out of equilibrium. *Journal of Statistical Mechanics: Theory and Experiment*, 2007(07):P07014, 2007.
- [46] Lorenzo Bertini, Alberto De Sole, Davide Gabrielli, Giovanni Jona-Lasinio, and Claudio Landim. Macroscopic fluctuation theory. *Reviews of Modern Physics*, 87(2):593, 2015.
- [47] Thierry Bodineau and Bernard Derrida. Distribution of current in nonequilibrium diffusive systems and phase transitions. *Physical Review E*, 72(6):066110, 2005.
- [48] T Bodineau, B Derrida, V Lecomte, and F Van Wijland. Long range correlations and phase transitions in non-equilibrium diffusive systems. *Journal of Statistical Physics*, 133:1013–1031, 2008.
- [49] T Bodineau and M Lagouge. Current large deviations in a driven dissipative model. *Journal of Statistical Physics*, 139(2):201–218, 2010.
- [50] AJ Bray, AJ McKane, and TJ Newman. Path integrals and non-markov processes. ii. escape rates and stationary distributions in the weak-noise limit. *Physical Review A*, 41(2):657, 1990.
- [51] Thomas Speck, Andreas M Menzel, Julian Bialké, and Hartmut Löwen. Dynamical mean-field

- theory and weakly non-linear analysis for the phase separation of active brownian particles. *The Journal of chemical physics*, 142(22), 2015.
- [52] John Cardy. Reaction-diffusion processes. *A + A*, 100(26):13–19, 2006.
- [53] David Landau and Kurt Binder. *A guide to Monte Carlo simulations in statistical physics*. Cambridge university press, 2021.
- [54] Nicolaas Godfried Van Kampen. *Stochastic processes in physics and chemistry*, volume 1. Elsevier, 1992.
- [55] Crispin W Gardiner et al. *Handbook of stochastic methods*, volume 3. springer Berlin, 1985.
- [56] Kay Jörg Wiese. Coherent-state path integral versus coarse-grained effective stochastic equation of motion: From reaction diffusion to stochastic sandpiles. *Physical Review E*, 93(4):042117, 2016.
- [57] Masao Doi. Second quantization representation for classical many-particle system. *Journal of Physics A: Mathematical and General*, 9(9):1465, 1976.
- [58] Luca Peliti. Path integral approach to birth-death processes on a lattice. *Journal de Physique*, 46(9):1469–1483, 1985.
- [59] Hans-Karl Janssen, Frédéric van Wijland, Olivier Deloubriere, and Uwe C Täuber. Pair contact process with diffusion: Failure of master equation field theory. *Physical Review E—Statistical, Nonlinear, and Soft Matter Physics*, 70(5):056114, 2004.
- [60] Soumyabrata Saha and Tridib Sadhu. Large deviations in the symmetric simple exclusion process with slow boundaries: A hydrodynamic approach. *arXiv preprint arXiv:2310.11350*, 2023.
- [61] Yongjoo Baek and Yariv Kafri. Singularities in large deviation functions. *Journal of Statistical Mechanics: Theory and Experiment*, 2015(8):P08026, 2015.
- [62] Alexei Andreanov, Giulio Biroli, Jean-Philippe Bouchaud, and Alexandre Lefevre. Field theories and exact stochastic equations for interacting particle systems. *Physical Review E*, 74(3):030101, 2006.
- [63] Alexandre Lefevre and Giulio Biroli. Dynamics of interacting particle systems: stochastic process and field theory. *Journal of Statistical Mechanics: Theory and Experiment*, 2007(07):P07024, 2007.
- [64] Benjamin Doyon, Gabriele Perfetto, Tomohiro Sasamoto, and Takato Yoshimura. Ballistic macroscopic fluctuation theory. *SciPost Physics*, 15(4):136, 2023.
- [65] Paul Cecil Martin, ED Siggia, and HA Rose. Statistical dynamics of classical systems. *Physical Review A*, 8(1):423, 1973.
- [66] Hans-Karl Janssen. On a lagrangean for classical field dynamics and renormalization group calculations of dynamical critical properties. *Zeitschrift für Physik B Condensed Matter*, 23(4):377–380, 1976.
- [67] C de Dominicis. Techniques de renormalisation de la théorie des champs et dynamique des phénomènes critiques. In *J. Phys., Colloq*, volume 37, page 247, 1976.
- [68] Tal Agranov, Michael E Cates, and Robert L Jack. Entropy production and its large deviations in an active lattice gas. *Journal of Statistical Mechanics: Theory and Experiment*, 2022(12):123201, 2022.
- [69] Tal Agranov, Sunghan Ro, Yariv Kafri, and Vivien Lecomte. Macroscopic fluctuation theory and current fluctuations in active lattice gases. *SciPost Physics*, 14(3):045, 2023.
- [70] Vlad Elgart and Alex Kamenev. Rare event statistics in reaction-diffusion systems. *Physical Review E*, 70(4):041106, 2004.
- [71] Vlad Elgart and Alex Kamenev. Classification of phase transitions in reaction-diffusion models. *Physical Review E*, 74(4):041101, 2006.
- [72] Alex Kamenev. *Field theory of non-equilibrium systems*. Cambridge University Press, 2023.
- [73] Tal Agranov, Sunghan Ro, Yariv Kafri, and Vivien Lecomte. Exact fluctuating hydrodynamics of active lattice gases—typical fluctuations. *Journal of Statistical Mechanics: Theory and Experiment*, 2021(8):083208, 2021.
- [74] Philip G Drazin. *Nonlinear systems*. Number 10. Cambridge University Press, 1992.

- [75] Mehran Kardar. *Statistical physics of fields*. Cambridge University Press, 2007.
- [76] Philip G Drazin. *Introduction to hydrodynamic stability*, volume 32. Cambridge university press, 2002.
- [77] Mark C Cross and Pierre C Hohenberg. Pattern formation outside of equilibrium. *Reviews of modern physics*, 65(3):851, 1993.
- [78] Pierre C Hohenberg and Bertrand I Halperin. Theory of dynamic critical phenomena. *Reviews of Modern Physics*, 49(3):435, 1977.
- [79] Lev Davidovich Landau and Evgenii Mikhailovich Lifshitz. *Statistical Physics: Volume 5*, volume 5. Elsevier, 2013.
- [80] Julien Tailleur, Jorge Kurchan, and Vivien Lecomte. Mapping nonequilibrium onto equilibrium: the macroscopic fluctuations of simple transport models. *Physical review letters*, 99(15):150602, 2007.
- [81] Julien Tailleur, Jorge Kurchan, and Vivien Lecomte. Mapping out-of-equilibrium into equilibrium in one-dimensional transport models. *Journal of Physics A: Mathematical and Theoretical*, 41(50):505001, 2008.
- [82] ME Cates and C Nardini. Classical nucleation theory for active fluid phase separation. *Physical Review Letters*, 130(9):098203, 2023.
- [83] Mattia Scandolo, Johannes Pausch, and Michael E Cates. Active ising models of flocking: A field-theoretic approach. *arXiv preprint arXiv:2306.10791*, 2023.
- [84] M Droz and A McKane. Equivalence between poisson representation and fock space formalism for birth-death processes. *Journal of Physics A: Mathematical and General*, 27(13):L467, 1994.
- [85] Benjamin Partridge and Chiu Fan Lee. Critical motility-induced phase separation belongs to the ising universality class. *Physical review letters*, 123(6):068002, 2019.
- [86] Claudio Maggi, Matteo Paoluzzi, Andrea Crisanti, Emanuela Zaccarelli, and Nicoletta Gnan. Universality class of the motility-induced critical point in large scale off-lattice simulations of active particles. *Soft Matter*, 17(14):3807–3812, 2021.
- [87] Florian Dittrich, Thomas Speck, and Peter Virnau. Critical behavior in active lattice models of motility-induced phase separation. *The European Physical Journal E*, 44:1–10, 2021.
- [88] Thomas Speck. Critical behavior of active brownian particles: Connection to field theories. *Physical Review E*, 105(6):064601, 2022.
- [89] Tomer Markovich, Étienne Fodor, Elsen Tjhung, and Michael E Cates. Thermodynamics of active field theories: Energetic cost of coupling to reservoirs. *Physical Review X*, 11(2):021057, 2021.
- [90] Udo Seifert. Stochastic thermodynamics, fluctuation theorems and molecular machines. *Reports on progress in physics*, 75(12):126001, 2012.
- [91] John W Negele. *Quantum many-particle systems*. CRC Press, 2018.
- [92] Michael E Cates, Étienne Fodor, Tomer Markovich, Cesare Nardini, and Elsen Tjhung. Stochastic hydrodynamics of complex fluids: Discretisation and entropy production. *Entropy*, 24(2):254, 2022.